

VidEdit: Zero-shot and Spatially Aware Text-driven Video Editing

Paul Couairon^{1,3} Clément Rambour² Jean-Emmanuel Haugeard³ Nicolas Thome¹

¹ Sorbonne Université, ISIR, Paris, France ² CNAM, CEDRIC, Paris, France

³ Thales SIX GTS France, Palaiseau, France



Figure 1: **VIDEDIT** allows to perform rich and diverse video edits on a precise semantic region of interest while perfectly preserving untargeted areas. The method is lightweight and maintains a strong temporal consistency on long-term videos.

Abstract

Recently, diffusion-based generative models have achieved remarkable success for image generation and edition. However, their use for video editing still faces important limitations. This paper introduces **VIDEDIT**, a novel method for zero-shot text-based video editing ensuring strong temporal and spatial consistency. Firstly, we propose to combine atlas-based and pre-trained text-to-image diffusion models to provide a training-free and efficient editing method, which by design fulfills temporal smoothness. Secondly, we leverage off-the-shelf panoptic segmenters along with edge detectors and adapt their use for conditioned diffusion-based atlas editing. This ensures a fine spatial control on targeted regions while strictly preserving the structure of the original video. Quantitative and qualitative experiments show that **VIDEDIT** outperforms state-of-the-art methods on DAVIS dataset, regarding semantic faithfulness, image preservation, and temporal consistency metrics. With this framework, processing a single video only takes approximately one minute, and it can generate multiple compatible edits based on a unique text prompt. Project Page: <https://videdit.github.io>

1 Introduction

Diffusion-based models [10, 33, 29, 27] have recently taken over image generation. Contrary to generative adversarial networks [7, 13, 40], they can be reliably trained on massive amounts of data and produce convincing samples. Besides, they can also be used for editing purposes by integrating conditional modalities such as text [29], edge maps or beyond [41, 23]. Such capacities have given rise to numerous methods that assist artists in their content creation endeavor [1, 34, 22, 15].

Yet, unlike image editing, text-based video editing represents a whole new challenge. Indeed, naive frame-wise application of text-driven diffusion models leads to flickering video results that look poor to the human eye as they lack motion information and 3D shape understanding. To overcome this challenge, numerous methods introduce diverse spatiotemporal attention mechanisms that aim to preserve objects' appearance across neighboring frames while respecting the motion dynamics [37, 25, 3, 36, 19]. However, they not only require substantial memory resources but also focus on a small number of frames as the proposed spatiotemporal attention mechanisms are not reliable enough over time to model long-term dependencies. On the other hand, current atlas-based video editing methods [2, 20] require costly optimization procedures for each target text query and do not enable precise spatial editing control nor produce diverse samples compatible with a unique text prompt.

This paper introduces VEDIT, a simple and effective zero-shot text-based video editing method that shows high temporal consistency and offers object-level control over the appearance of the video content. The rationale of the approach is shown in Fig 1. Given an input video and a target editing request, e.g. "road" \rightarrow "a night sky", VEDIT modifies the original content by precisely delineating the regions of interest, leaving the rest of the video unaltered, and ensuring a high temporal consistency. To achieve this goal, the approach includes two main contributions.

Firstly, we combine the strengths of atlas-based approaches and text-to-image diffusion models. The idea is to decompose videos into a set of layered neural atlases [14] which are designed to provide an interpretable and semantic unified representation of the content. We then apply a pre-trained text-driven image diffusion model to perform zero-shot atlas editing, the temporal coherence being preserved when edits are mapped back to the original frames. Consequently, the approach is *training free* and efficient as it can edit a full video in about one minute.

In addition, we take special care to preserve the structure and geometry in the atlas space as it not only encodes objects' temporal appearance but also their movements and spatial placement in the image space. Therefore, to constrain the edits to match as accurately as possible the semantic layout of an atlas representation, we leverage an off-the-shelf panoptic segmenter [4] as well as an edge detection model (HED) [38]. The segmenter extracts the regions of interest whereas the HED specifies the inner and outer edges that guide the editing process for an optimal video content alteration/preservation trade-off. Hence, we adapt the utilization of a spatially grounded editing method to a conditional diffusion process that operates on atlas representations. This is achieved by extracting a crop around the area of interest and intentionally utilizing a non-invertible noising process.

We conduct extensive experiments on DAVIS dataset, providing quantitative and qualitative comparisons with respect to video baselines based or not on atlas representations, and frame-based editing methods. We show that VEDIT outperforms these baselines in terms of semantic matching to the target text query, original content preservation, and temporal consistency. Especially, we highlight the benefits of our approach for foreground or background object editions. We also illustrate the importance of the proposed contributions for optimal performance. Finally, we show the efficiency of VEDIT and its capacity to generate diverse samples compatible with a given text prompt.

2 Related Work

Text-driven Image Editing. In the past few years, Text-to-Image (T2I) generation has become an increasingly hot topic. Recently, these generative models have benefited from the swelling popularity of diffusion models [10, 33, 27] as well as the accurate image-text alignment provided by CLIP [26]. Latent Diffusion Models (LDMs) [29] propose to enhance the training efficiency, memory, and runtime of such models, by taking the diffusion process into the latent space of an autoencoder. As a result, they have taken over text-driven image generation and editing. For example, SEdit [21] proposes to corrupt an image by adding Gaussian noise, and a text-conditioned diffusion network denoises it to generate new content. Other works aim to perform local image editing by using an edit

mask [1, 5] and combining the features of each step in the generation process for image blending. Still focusing on image-to-image translation, [8] or [34] extract attention features to constrain the editions to regions of interest. [15] or [22] refine image editing via an optimization procedure.

Text-driven Video Editing. While significant advances have been made in T2I generation, modeling strong temporal consistency for video generation and editing is still a labor in progress. Several works aim to generate new video content directly from an input text query with novel spatiotemporal attention mechanisms [12, 11, 35, 32, 43]. However, these methods still suffer from annoying flickering artifacts and inconsistencies. Video editing lies at the intersection of image editing and video generation. Yet, a naive frame-wise application of image editing models to a video produces unsatisfactory results due to the lack of temporal awareness. Based on neural layered atlases [14], Text2Live [2] allows coherent text-to-video (T2V) editing but its training procedure for each prompt makes it impractical to use. Also based on neural atlases, [17] aims to handle shape changes in video editing. Contrary to [17], we focus on editing objects while preserving their overall shapes. Gen-1 [6] proposes a video diffusion model trained on a large-scale dataset of uncaptioned videos and paired text-image data. Tune-A-Video [37] overfits a video on a given text query and can then generate new content from similar prompts. Other approaches [19, 25, 31, 3, 36] propose diverse spatiotemporal attention mechanisms to transfer pre-trained text-to-image model knowledge to text-to-video. However, not only are their spatio-temporal attention mechanisms not reliable enough to handle long-term coherence, but they tend to deteriorate the original video content.

3 VidEdit Framework

Video editing often requires substantial modification of specific objects. The ergonomony and performance of text-conditioned diffusion models are a great motivation to perform those editions based on text queries. To this end, we introduce VIDEIT, a novel lightweight, and consistent video editing framework that provides object-scale control over the video content. The main steps of VIDEIT are illustrated in Fig. 2. First, we propose to benefit from Neural Layered Atlas (NLA) [14] to build global representations of the video content ensuring strong spatial and temporal coherence. Second, the underlying global scene encoded in the atlas representation is processed through a zero-shot image editing diffusion procedure. Text-based editing inherently faces the difficulty of accurately identifying the region to edit from the input text and may as well deteriorate neighboring regions or introduce rough deformations in the object aspect [37, 3, 19]. We avoid these pitfalls by carefully extracting rich semantic information using HED maps and off-the-shelf segmentation models [4] to guide the diffusion generative process. We adapt their design and utilization for atlas images.

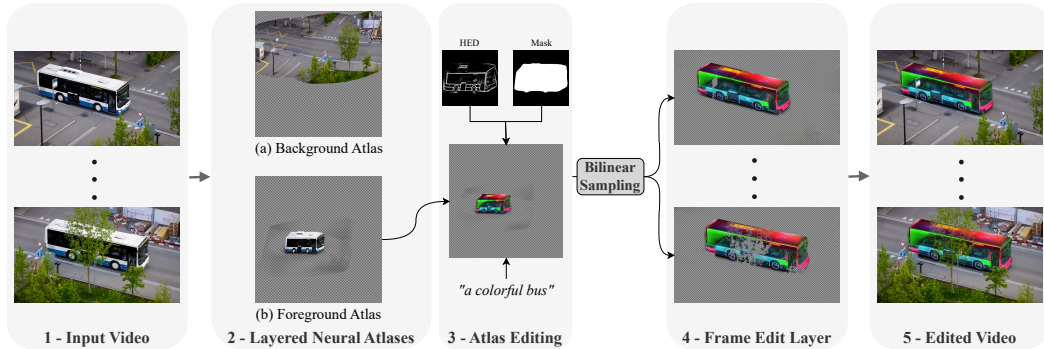


Figure 2: **Our VIDEIT pipeline:** An input video (1) is fed into NLA models which learn to decompose it into 2D atlases (2). Depending on the object we want to edit, we select an atlas representation onto which we apply our editing diffusion pipeline (3). The edited atlas is then mapped back to frames via a bilinear sampling from the associated pre-trained network \mathbb{M} (4). Finally, the frame edit layers are composited over the original frames to obtain our desired edited video (5).

3.1 Zero-shot Atlas-based video editing

Neural Layered Atlases. Neural Layered Atlases (NLA) [14] provide a unified 2D representation of the appearance of an object or the background through time, by decomposing a video into a set

of 2D atlases. Formally, each pixel location $p = (x, y, t) \in \mathbb{R}^3$ is fed into three mapping networks. While \mathbb{M}_f and \mathbb{M}_b map p to a 2D (u, v) -coordinate in the foreground and background atlas regions respectively, \mathbb{M}_α predicts a foreground opacity value:

$$\mathbb{M}_b(p) = (u_b^p, v_b^p), \quad \mathbb{M}_f(p) = (u_f^p, v_f^p), \quad \mathbb{M}_\alpha(p) = \alpha^p$$

Each of the predicted (u, v) -coordinates are then fed into an atlas network \mathbb{A} , which yields an RGB color at that location. Color can then be reconstructed by alpha-blending the predicted foreground c_f^p and background c_b^p colors at each position p , according to the corresponding opacity value α^p :

$$c^p = (1 - \alpha^p)c_b^p + \alpha^p c_f^p.$$

We train NLA in a self-supervised manner as in [14]. The obtained background and foreground atlases are large 2D pixel representations disentangling the layers from the video. By utilizing these mapping and opacity networks, one can edit the RGBA pixel values and project them back onto the original video frames.

Zero-shot atlas editing. The 2D atlases obtained by disentangling the video are a well-posed framework to edit objects while ensuring a strong temporal consistency. We propose here to perform zero-shot text-based editing of atlas images. This is in sharp contrast with [2], which requires training a specific generative model for each target text query. We use a pre-trained conditioned latent diffusion model, although our approach is agnostic to the image editing tool. As illustrated with Fig. 2, the automatic video editing charge is cast into a much simpler, training free, and maneuverable image editing task that leads to competitive performance.

3.2 Semantic Atlas Editing with VIDEIT

2D atlas representations pave the way to use powerful off-the-shelf segmentation models [39, 16, 44] to precisely circumscribe the regions-of-interest. The results are then clean object-level editions maximizing the consistency with the original video and the rendering of the targeted object. In addition, we also extract HED maps as they lead to rich object descriptions. We then use the extracted masks to guide the generative process of a DDIM (Denoising Diffusion Implicit Model) model conditioned by both a target prompt and a HED map, the latter ensuring to preserve the semantic structure of the source image. The whole pipeline is illustrated in Fig. 3.

Step 1: Extracting precise spatial information. In order to generate edits that are meaningful and realistic once mapped back in the original image space, we have to guide the generative process toward a plausible output in the atlas representation. Our objective is then twofold. First, we want to precisely localize our region of interest in the atlas in order to only make alterations within this area. As in [1], this edit mask will help to seamlessly blend our edits in the video content while having minimal impact on out-of-interest parts of the video. Recently, [5] proposed a method to automatically infer such a mask with a reference and target text queries, but it generally overshoots the region that requires to be edited, compromising the integrity of the original video content. On the other hand, segmentation models have recently seen spectacular advances [4, 39, 16, 44], allowing to confidently and accurately detect and recognize objects in images. When applied directly onto atlas grids, we observe that, despite the distribution shift with real-world images, these models generalize sufficiently well to infer a mask around the targeted regions. Consequently, we choose to leverage the performance of these frameworks to perform panoptic segmentation and thus gain object-level spatial control over our future edits. Hence, we first take our original atlas representation which is composed of an RGB image and an alpha channel. In order to assist the segmentation network in providing a precise mask, we mix the RGB image with a fully white patch according to the alpha values. This step allows to enhance the contrast between the object and the background as illustrated in Supplementary D. Then, we identify the object or region that we need to locate and create a bounding box around the identified area. Finally, we produce a more accurate mask M on this smaller patch.

Second, as we are interested in changing the aspect of objects while preserving their overall shapes, we have to ensure that our edits match their semantic structure in the atlas representation. Several works propose methods to perform image-to-image translation [22, 34, 2, 8]. However, their various drawbacks in terms of editing time or lack of generalization on atlas representations that are too far away from real-world images, hinder the use of such approaches directly in the atlas space. Consequently, we choose to align the internal knowledge of a generative text-to-image model with an

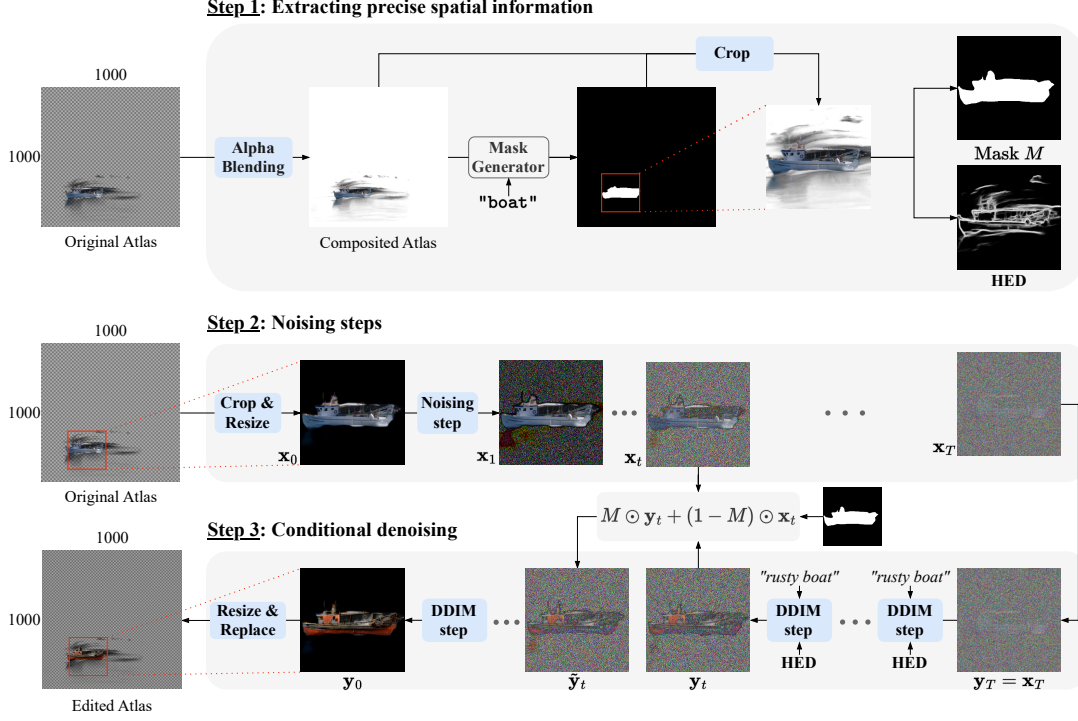


Figure 3: The three steps of our atlas editing procedure.

external control signal that helps preserving the semantic structure of objects. To this end, we opt to exploit the accurate and computationally efficient HED algorithm [38] to bring out critical edges that characterize the structure of our image.

Step 2: Noising steps. We crop a patch from the original atlas at the same location as we did to obtain our conditional information. Different from [5], we choose not to perform inverse DDIM in the latent space to encode \mathbf{x}_0 for two main reasons. First, the inverting procedure is relatively time-consuming. We thus opt to limit the computational overhead in order to increase our editing efficiency. Second, we search for a probabilistic method that can generate a range of editing options suitable for a given text prompt. This requirement eliminates DDIM as a viable option since it operates deterministically and does not offer the desired diversity in outputs. As a result, starting from \mathbf{x}_0 , we decide to use a classical noising procedure for T_{max} steps, which leads to a nearly isotropic Gaussian noise sample $\mathbf{x}_{T_{max}}$, i.e. $p_\theta(\mathbf{x}_{T_{max}}) = \mathcal{N}(\mathbf{0}, \mathbf{I})$. We denote ρ the noising ratio such that $\rho = T/T_{max}$.

Step 3: Decoding with mask guidance. Our proposed method aims to condition a stable diffusion generation model using text prompts and HED maps. We adopt a modified version of the baseline diffusion model architecture, incorporating semantic guidance based on high-resolution semantic masks. Inspired by [1], we propose to directly blend our edits in our smaller input patch. Starting from our latent $\mathbf{y}_T = \mathbf{x}_T$, we decode it with a pre-trained diffusion model. At each step, we perform a single DDIM step [33], that denoises the latent in a direction determined by both the target prompt and the HED edge map:

$$\mathbf{y}_{t-1} = \sqrt{\alpha_{t-1}} \left(\frac{\mathbf{y}_t - \sqrt{1 - \alpha_t} \epsilon_\theta(\mathbf{y}_t, t, \mathbf{c}_p, \mathbf{c}_h)}{\sqrt{\alpha_t}} \right) + \sqrt{1 - \alpha_{t-1}} \epsilon_\theta(\mathbf{y}_t, t, \mathbf{c}_p, \mathbf{c}_h) \quad (1)$$

where \mathbf{c}_p and \mathbf{c}_h correspond to embeddings of the query text prompt and HED map, projected into a common representation space with \mathbf{y}_t , through dedicated cross-attention blocks. The encoder of the denoising U-Net ϵ_θ is applied separately on \mathbf{y}_t , the input to be denoised, and the HED conditioning $\mathbf{c}_h(\lambda)$ with λ a balancing coefficient that the decoder takes at each stage to compute a weighted sum of the activation maps.

The marginal of the forward process sample at step $t - 1$ admits a simple closed form given by $\mathbf{x}_{t-1} = \sqrt{\bar{\alpha}_{t-1}}\mathbf{x}_0 + \sqrt{1 - \bar{\alpha}_{t-1}}\epsilon_{t-1}$. We use this relation to retrieve the area outside the object’s mask during the generation process while the interior region is obtained following the standard diffusion process given in Eq. (1):

$$\tilde{\mathbf{y}}_{t-1} = M \odot \mathbf{y}_{t-1} + (1 - M) \odot \mathbf{x}_{t-1} \quad (2)$$

In the last step, the entire region outside the mask is replaced with the corresponding region from the input image, allowing to preserve exactly the background from the original crop. Our edited patch is finally replaced at its location within the atlas grid. Therefore, this pipeline seamlessly fuse the edited region with the unchanged parts of an atlas. Lastly, the edited atlas is used to perform bilinear sampling of frame edit layers. Once these layers are composited with their corresponding original frames, they produce an edited video that exhibits both spatial and temporal consistency.

4 Experiments

In this section, we describe our experimental setup, followed by qualitative and quantitative results.

4.1 Experimental setup

Dataset. Following [2, 37, 25], we evaluate our approach on videos from DAVIS dataset [24] resized at a 768×432 resolution. The length of these videos ranges from 20 to 70 frames. To automatically create edit prompts, we use a captioning model [18] to obtain descriptions of the original video content and we manually design 4 editing prompts for each video.

VidEdit setup. Our experiments are based on latent diffusion models [29]. We use a version of stable diffusion trained with HED edge detection [41] at a 512×512 resolution on LAION-5B dataset [30]. We choose Mask2former [4] as our instance segmentation network. To edit an atlas, we sample pure Gaussian noise (*i.e.* $\rho = 1$) and denoise it for 50 steps with DDIM sampling and classifier-free guidance [9]. For a single 70 frames video, it takes ~ 15 seconds to edit a 512×512 patch in an atlas and ~ 1 minute to reconstruct the video with the edit layer on a NVIDIA TITAN RTX. We set up the HED strength λ to 1 by default.

Baselines. We compare our method with two text-to-image frame-wise editing approaches and three text-to-video editing baselines. (1) *SDEdit* [21] is a framewise zero-shot editing approach that corrupts an input frame with noise and denoise it with a target text prompt. (2) *ControlNet* [41] performs frame-wise editing with an external condition extracted from the target frame. (3) *Text2Live* [2] is a Neural Layered Atlas (NLA) based method that trains a generator for each text query to optimize a CLIP-based loss. (4) *Tune-a-Video* (TAV) [37] fine-tunes an inflated version of a pre-trained diffusion model on a video to produce similar content. (5) *Pix2Video* [3] uses a structure-guided image diffusion model to perform text-guided edits on a key frame and propagate the changes to the future frames via self-attention feature injection.

Metrics. A video edit is expected (1) to faithfully render a target text query, (2) to preserve out-of-interest regions unaltered and (3) to be temporally consistent. First, in order to evaluate the faithfulness of an edit, we report semantic metrics computed with ViT-L/14 CLIP [26]. **Prompt Consistency** ($\mathcal{C}_{\text{Prompt}}$) measures the CLIP similarity between a text query and each video frame. **Frame Accuracy** ($\mathcal{A}_{\text{Frame}}$) corresponds to the percentage of edited frames that have a higher CLIP similarity with the target prompt than with the source caption. **Directional Similarity** (\mathcal{S}_{Dir}) quantifies how closely the alterations made to an original image align with the changes between a source caption and a target caption. Second, we evaluate original content preservation with image similarity metrics: **LPIPS** [42], **HaarPSI** [28] and **PSNR**. While LPIPS evaluates the perceptual similarity between two images in a deep feature space, HaarPSI performs a Haar wavelet decomposition to assess local similarities. On the contrary, PSNR measures the distance with an original image in the pixel space. Finally, we assess the temporal consistency with **Frame Consistency** ($\mathcal{C}_{\text{Frame}}$) that measures the CLIP similarity between consecutive video frames. We also provide an **Aggregate score** for semantic and similarity metrics that reflect the overall performance of each model on these aspects. More details on these metrics are provided in Supplementary A.

4.2 State-of-the-art comparison

Quantitative results. Table 1 gathers the overall comparison with respect to the chosen baselines¹. We observe that VIDEIT outperforms other approaches in terms of both semantic and similarity metrics. Moreover, it demonstrates better temporal consistency compared to other methods. Additionally, when comparing the processing time of different baselines, we found that VIDEIT has a significant advantage, with a ~ 30 -fold speed-up factor over Text2Live. We further illustrate the lightweight aspect of our method in Supplementary E. Regarding semantic metrics, as indicated by our best directional similarity score, VIDEIT performs highly consistent edits with respect to the change between the target text query and the source caption. Even though our method is close to Text2Live in terms of frame accuracy and prompt consistency, the latter explicitly optimizes a generator on a CLIP-based loss, making the aforementioned metrics not reliable to assess its generalization performance and editing quality, as will be shown in the qualitative results. When it comes to image preservation evaluated with our similarity metrics, VIDEIT outperforms all baselines in LPIPS and HaarPSI, and is similar to Text2Live on PSNR. This shows the capacity of our approach to optimally preserve the visual content of the source video while generating faithful edits to the target queries. Finally, VIDEIT outperforms all methods in C_{Frame} , and shows that the fine spatial control of our approach also translates in an improved temporal consistency.

Table 1: **State-of-the-art comparison.**

Method	Semantic				Similarity				Temporal	Time
	C_{Prompt} (\uparrow)	A_{Frame} (\uparrow)	S_{Dir} (\uparrow)	Agg. Score (\downarrow)	LPIPS (\downarrow)	HaarPSI (\uparrow)	PSNR (\uparrow)	Agg. Score (\downarrow)	C_{Frame} (\uparrow)	<i>min</i>
VidEdit (ours)	28.1 (± 3.0)	91.5 (± 1.1)	21.7 (± 8.4)	3.06	0.077 (± 0.054)	0.730 (± 0.109)	22.6 (± 3.6)	3.01	97.4 (± 1.4)	118
Text2Live [2]	28.7 (± 2.8)	94.1 (± 14.6)	20.4 (± 6.0)	3.07	0.155 (± 0.035)	0.710 (± 0.088)	22.8 (± 2.9)	4.04	97.0 (± 1.4)	3780
ControlNet [41]	28.0 (± 2.6)	84.8 (± 24.0)	18.7 (± 6.6)	3.30	0.647 (± 0.061)	0.312 (± 0.036)	10.8 (± 1.5)	12.85	86.2 (± 3.6)	561
SDEdit [21]	26.1 (± 2.9)	65.7 (± 31.8)	14.2 (± 7.4)	3.96	0.490 (± 0.051)	0.377 (± 0.034)	17.9 (± 1.6)	9.57	83.9 (± 5.2)	303
TAV [37]	27.5 (± 3.1)	73.4 (± 36.3)	13.7 (± 9.0)	3.92	0.584 (± 0.079)	0.274 (± 0.060)	13.0 (± 2.1)	12.00	96.4 (± 1.6)	274
Pix2Video [3]	29.0 (± 3.0)	82.9 (± 30.0)	16.2 (± 9.2)	3.47	0.540 (± 0.079)	0.326 (± 0.069)	13.8 (± 2.1)	10.90	94.4 (± 2.1)	252

To further analyze the fine-grained editing capacity of our method while preserving the original video content, we display for all baselines in Fig. 4, their local A_{Frame} score computed within a ground truth mask compared to an outer LPIPS metric (denoted O-LPIPS) computed on the invert of the mask². We see that VIDEIT reaches a very good local frame accuracy, even outperforming Text2Live. Moreover, VIDEIT shows a huge improvement on the O-LPIPS metric compared to the baselines, including Text2Live (3 vs 8), showing clearly a better preservation of out-of-interest regions.

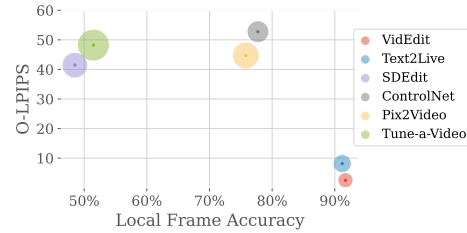


Figure 4: **Masked LPIPS vs Local Object Accuracy**

Qualitative results. We show in Fig. 5 a visual comparison against the baselines to qualitatively assess the improvement brought out by our method. We can see that VIDEIT performs fine-grained editing while perfectly preserving out-of-interest regions. In comparison to other baselines, the edits generated are more visually appealing and realistic. For example, VIDEIT obtains a frame accuracy (A_{Frame}) and prompt consistency (C_{Prompt}) scores of 26.5 and 30 respectively compared to Text2Live which reaches 26 and 35 respectively. However, we can see that Text2Live’s scores do not automatically translate into high-quality edits it often struggles to render detailed textures precisely localized on targeted regions. For example, ice creams are poorly rendered and some untargted areas are being altered. Regarding Tune-a-Video and Pix2Video baselines, the methods are unable to generate a faithful edit at the exact location and completely degrade the original content. Despite relatively high frame consistency scores in this video (96% for Tune-a-Video and 89% for Pix2Video vs 97.5% for VIDEIT), noticeable flickering artifacts undermine the video content. On the other hand, naive frame-wise application of image-to-image translation methods also leads to temporally inconsistent results. For example, SDEdit is unable to both generate a faithful edit and to preserve the original content as it inherently faces a trade-off between the two. Other visual comparisons are shown in Supplementary C.

¹Results in bold correspond to the best methods based on a paired t -test (risk 5%).

²The size of each dot is proportional to the local frame accuracy’s standard deviation.

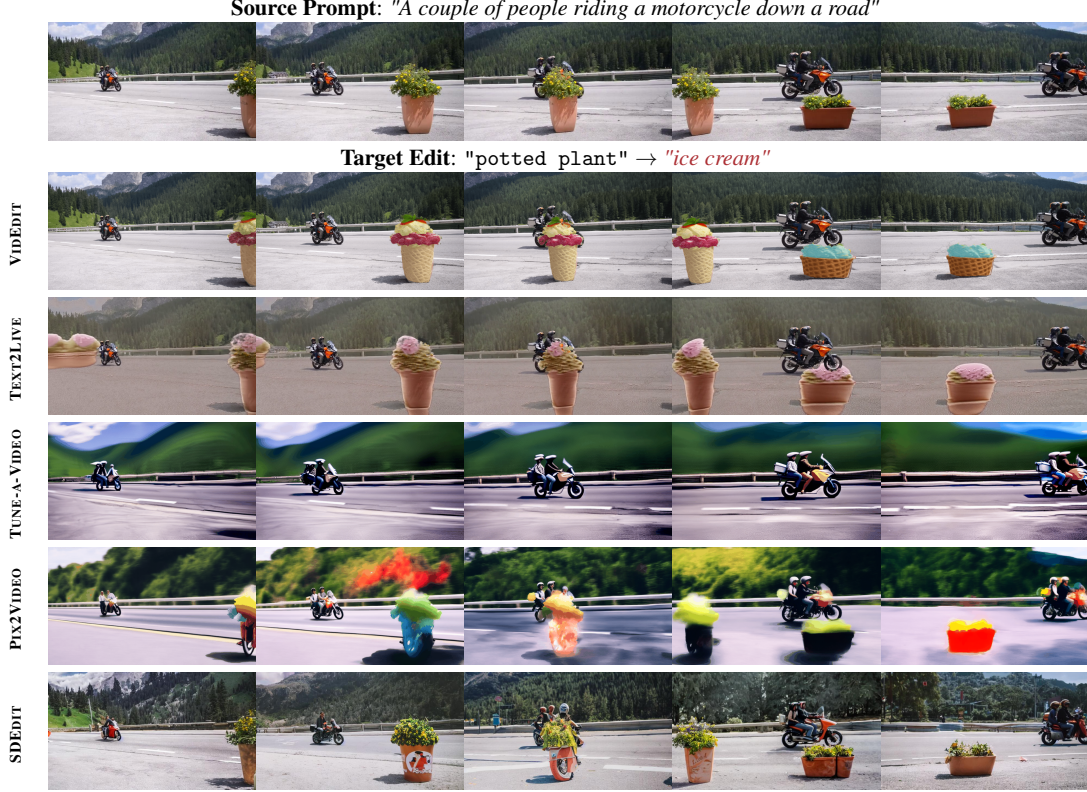


Figure 5: **Qualitative comparison of VIDEIT with other baselines.** VIDEIT generates higher quality textures than Text2Live. Tune-a-Video and Pix2video completely alters untargeted regions.

4.3 Model Analysis

Ablations. We perform ablation studies to demonstrate the importance of our conditional controls once we map the edits back to the original image space. Tab. 2 compares the performance of our editing pipeline with both instance mask segmentation and HED edge conditioning against scenarios where these controls are disabled.

In the case where no conditional control is passed on to the model, we observe a substantial drop in semantic metrics as the model generates edits at random locations in the atlas whose shapes don't match the structure of the target object. The introduction of edge conditioning without spatial awareness is quite similar to the previous case with the difference that the model tries to locally match the control information. This results in slightly better semantic results and similarity metrics than with no edge control. Finally, blending an edit with mask control without taking structure conditioning into account generates an edit at the right location but that is semantically incoherent once mapped back to the original images. Yet, this scenario achieves a decent prompt consistency as the objects still correspond to the target text query. We provide a visual illustration of this ablation study in Supplementary B.

Table 2: **Ablation study.** The mask and the HED map help to generate meaningful edits once mapped back in the original frame space.

Controls		Semantic metrics			Similarity metrics		
Mask	HED	$\mathcal{C}_{\text{Prompt}}$ (\uparrow)	$\mathcal{A}_{\text{Frame}}$ (\uparrow)	\mathcal{S}_{Dir} (\uparrow)	LPIPS (\downarrow)	HaarPSI (\uparrow)	PSNR (\uparrow)
✓	✓	28.1 (± 3.0)	91.5 (± 11.1)	21.7 (± 8.4)	0.077 (± 0.054)	0.730 (± 0.109)	22.6 (± 3.6)
✗	✗	25.5 (± 3.1)	64.3 (± 38.3)	10.6 (± 7.5)	0.099 (± 0.051)	0.632 (± 0.131)	20.1 (± 4.0)
✗	✓	26.3 (± 3.0)	72.4 (± 34.0)	13.0 (± 7.6)	0.095 (± 0.049)	0.672 (± 0.110)	20.8 (± 3.6)
✓	✗	27.5 (± 2.8)	81.9 (± 24.2)	18.0 (± 8.4)	0.081 (± 0.042)	0.639 (± 0.128)	20.7 (± 3.3)

Impact of hyperparameters. We analyze in Fig. 6 VIDEIT's behaviour versus the HED conditioning strength and noising ratio, respectively λ and ρ . To analyze the trade-off between semantic

editing and source image preservation, we compute a local LPIPS computed within a ground-truth mask, provided by DAVIS, versus a local CLIP score computed within the same mask for an edited object.

On the left panel, we can see that for λ values lower than 0.4, the edge conditioning is not strong enough to guide the edits toward a plausible output on the video frames. This phenomenon is illustrated in Supplementary B. On the contrary, for strength values larger than 1.2, the conditioning weighs too much on the model and hinders its ability to generate faithful edits. As expected, we notice that the local LPIPS decreases as the edge conditioning increases.

While the decreasing rate is substantial between 0 and 1, the marginal gain diminishes for larger values. Overall, setting the HED strength between 0.8 and 1.2 robustly enables to both perform faithful edits and preserve the original content. On the right panel, we see that both local CLIP score and LPIPS increase with the noising ratio. Indeed, for a null ρ value, the region is reconstructed from the atlas, nearly identically to the original, and is then rewarded a low LPIPS. However, as no modification has been performed, the patch does not match the target text query and gets a lower CLIP score. As the noising ratio increases, the region deviates more from the input but also better matches the target edit. Note that for a ρ value of 100%, the local LPIPS is constrained below 19, which still indicates a low disparity with the original image.

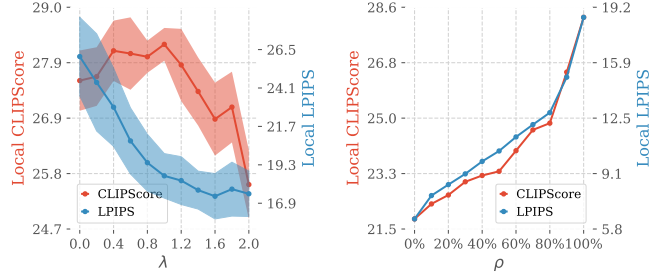


Figure 6: VIDEIT behavior wrt. different λ and ρ values.

Diversity. Finally, we illustrate in Fig. 7 the capacity of VIDEIT to produce various and sundry video edits from a unique pair (*video*; *target text query*). In contrast, the randomness in Text2Live’s training process only comes from the generator’s weights initialization. As a result, method converges towards a unique solution and thus shows poor diversity in the generated samples.



Figure 7: **Texture diversity.** We edit each video four times with the same input text query. Compared to Text2Live, our method is able to synthesize more diverse samples in much less time.

5 Conclusion & Discussion

We introduced VIDEIT, a lightweight algorithm for zero-shot semantic video editing based on latent diffusion models. We have shown experimentally that this approach conserves more appearance information from the input video than other diffusion-based methods, leading to lighter edits. Nevertheless, the approach has a few limitations. Common with [14], the capacity of the MLP mapping networks decreases for complex videos involving rapid movements and very long-term videos. Since our method relies on the quality of such atlas representations, one possible way to expand the scope of possible video edits would be to strengthen and robustify the neural layered atlases construction approach. Finally, video editing raises several ethical challenges that we discuss here. Open-source diffusion models are trained on large amounts of data and inherit their biases. Therefore, the use of such models can raise ethical issues, whether the target text prompt is intentionally harmful or not. In addition, video editing algorithms could be used with harmful intent such as harassment or propagating fake news. To mitigate potential misuse, the Stable Diffusion model is released under a license focused on ethical and legal use, stating explicitly that users “must not distribute harmful, offensive, dehumanizing content or otherwise harmful representations of people or their environments, cultures, religions, etc. produced with the model weights”.

References

- [1] Omri Avrahami, Dani Lischinski, and Ohad Fried. Blended diffusion for text-driven editing of natural images. In *2022 IEEE/CVF Conference on Computer Vision and Pattern Recognition (CVPR)*. IEEE, jun 2022. doi: 10.1109/cvpr52688.2022.01767. URL <https://doi.org/10.1109%2Fcvpr52688.2022.01767>.
- [2] Omer Bar-Tal, Dolev Ofri-Amar, Rafail Fridman, Yoni Kasten, and Tali Dekel. Text2live: Text-driven layered image and video editing. In *Computer Vision—ECCV 2022: 17th European Conference, Tel Aviv, Israel, October 23–27, 2022, Proceedings, Part XV*, pages 707–723. Springer, 2022.
- [3] Duygu Ceylan, Chun-Hao Paul Huang, and Niloy J Mitra. Pix2video: Video editing using image diffusion. *arXiv preprint arXiv:2303.12688*, 2023.
- [4] Bowen Cheng, Ishan Misra, Alexander G Schwing, Alexander Kirillov, and Rohit Girdhar. Masked-attention mask transformer for universal image segmentation. In *Proceedings of the IEEE/CVF Conference on Computer Vision and Pattern Recognition*, pages 1290–1299, 2022.
- [5] Guillaume Couairon, Jakob Verbeek, Holger Schwenk, and Matthieu Cord. Diffedit: Diffusion-based semantic image editing with mask guidance. *arXiv preprint arXiv:2210.11427*, 2022.
- [6] Patrick Esser, Johnathan Chiu, Parmida Atighehchian, Jonathan Granskog, and Anastasis Germanidis. Structure and content-guided video synthesis with diffusion models. *arXiv preprint arXiv:2302.03011*, 2023.
- [7] Ian Goodfellow, Jean Pouget-Abadie, Mehdi Mirza, Bing Xu, David Warde-Farley, Sherjil Ozair, Aaron Courville, and Yoshua Bengio. Generative adversarial networks. *Communications of the ACM*, 63(11):139–144, 2020.
- [8] Amir Hertz, Ron Mokady, Jay Tenenbaum, Kfir Aberman, Yael Pritch, and Daniel Cohen-Or. Prompt-to-prompt image editing with cross attention control. *arXiv preprint arXiv:2208.01626*, 2022.
- [9] Jonathan Ho and Tim Salimans. Classifier-free diffusion guidance. *arXiv preprint arXiv:2207.12598*, 2022.
- [10] Jonathan Ho, Ajay Jain, and Pieter Abbeel. Denoising diffusion probabilistic models. *Advances in Neural Information Processing Systems*, 33:6840–6851, 2020.
- [11] Jonathan Ho, William Chan, Chitwan Saharia, Jay Whang, Ruiqi Gao, Alexey Gritsenko, Diederik P Kingma, Ben Poole, Mohammad Norouzi, David J Fleet, et al. Imagen video: High definition video generation with diffusion models. *arXiv preprint arXiv:2210.02303*, 2022.
- [12] Jonathan Ho, Tim Salimans, Alexey Gritsenko, William Chan, Mohammad Norouzi, and David J Fleet. Video diffusion models. *arXiv preprint arXiv:2204.03458*, 2022.
- [13] Tero Karras, Samuli Laine, and Timo Aila. A style-based generator architecture for generative adversarial networks. *2019 IEEE/CVF Conference on Computer Vision and Pattern Recognition (CVPR)*, pages 4396–4405, 2018.
- [14] Yoni Kasten, Dolev Ofri, Oliver Wang, and Tali Dekel. Layered neural atlases for consistent video editing. *ACM Transactions on Graphics (TOG)*, 40(6):1–12, 2021.
- [15] Bahjat Kavar, Shiran Zada, Oran Lang, Omer Tov, Huiwen Chang, Tali Dekel, Inbar Mosseri, and Michal Irani. Imagic: Text-based real image editing with diffusion models. *arXiv preprint arXiv:2210.09276*, 2022.
- [16] Alexander Kirillov, Eric Mintun, Nikhila Ravi, Hanzi Mao, Chloe Rolland, Laura Gustafson, Tete Xiao, Spencer Whitehead, Alexander C. Berg, Wan-Yen Lo, Piotr Dollár, and Ross B. Girshick. Segment anything. *ArXiv*, abs/2304.02643, 2023.
- [17] Yao-Chih Lee, Ji-Ze Genevieve Jang, Yi-Ting Chen, Elizabeth Qiu, and Jia-Bin Huang. Shape-aware text-driven layered video editing. *arXiv e-prints*, pages arXiv–2301, 2023.

- [18] Junnan Li, Dongxu Li, Caiming Xiong, and Steven Hoi. Blip: Bootstrapping language-image pre-training for unified vision-language understanding and generation. In *International Conference on Machine Learning*, pages 12888–12900. PMLR, 2022.
- [19] Shaoteng Liu, Yuechen Zhang, Wenbo Li, Zhe Lin, and Jiaya Jia. Video-p2p: Video editing with cross-attention control. *arXiv preprint arXiv:2303.04761*, 2023.
- [20] Sebastian Loeschke, Serge J. Belongie, and Sagie Benaim. Text-driven stylization of video objects. In *ECCV Workshops*, 2022.
- [21] Chenlin Meng, Yutong He, Yang Song, Jiaming Song, Jiajun Wu, Jun-Yan Zhu, and Stefano Ermon. Sdedit: Guided image synthesis and editing with stochastic differential equations. In *International Conference on Learning Representations*, 2021.
- [22] Ron Mokady, Amir Hertz, Kfir Aberman, Yael Pritch, and Daniel Cohen-Or. Null-text inversion for editing real images using guided diffusion models. *arXiv preprint arXiv:2211.09794*, 2022.
- [23] Chong Mou, Xintao Wang, Liangbin Xie, Jing Zhang, Zhongang Qi, Ying Shan, and Xiaoju Qie. T2i-adapter: Learning adapters to dig out more controllable ability for text-to-image diffusion models. *ArXiv*, abs/2302.08453, 2023.
- [24] Jordi Pont-Tuset, Federico Perazzi, Sergi Caelles, Pablo Arbeláez, Alex Sorkine-Hornung, and Luc Van Gool. The 2017 davis challenge on video object segmentation. *arXiv preprint arXiv:1704.00675*, 2017.
- [25] Chenyang Qi, Xiaodong Cun, Yong Zhang, Chenyang Lei, Xintao Wang, Ying Shan, and Qifeng Chen. Fatezero: Fusing attentions for zero-shot text-based video editing. *arXiv preprint arXiv:2303.09535*, 2023.
- [26] Alec Radford, Jong Wook Kim, Chris Hallacy, Aditya Ramesh, Gabriel Goh, Sandhini Agarwal, Girish Sastry, Amanda Askell, Pamela Mishkin, Jack Clark, et al. Learning transferable visual models from natural language supervision. In *International conference on machine learning*, pages 8748–8763. PMLR, 2021.
- [27] Aditya Ramesh, Prafulla Dhariwal, Alex Nichol, Casey Chu, and Mark Chen. Hierarchical text-conditional image generation with clip latents. *arXiv preprint arXiv:2204.06125*, 2022.
- [28] Rafael Reisenhofer, Sebastian Bosse, Gitta Kutyniok, and Thomas Wiegand. A haar wavelet-based perceptual similarity index for image quality assessment. *Signal Processing: Image Communication*, 61:33–43, 2018. ISSN 0923-5965. doi: <https://doi.org/10.1016/j.image.2017.11.001>. URL <https://www.sciencedirect.com/science/article/pii/S0923596517302187>.
- [29] Robin Rombach, Andreas Blattmann, Dominik Lorenz, Patrick Esser, and Björn Ommer. High-resolution image synthesis with latent diffusion models. In *Proceedings of the IEEE/CVF Conference on Computer Vision and Pattern Recognition*, pages 10684–10695, 2022.
- [30] Christoph Schuhmann, Romain Beaumont, Richard Vencu, Cade Gordon, Ross Wightman, Mehdi Cherti, Theo Coombes, Aarush Katta, Clayton Mullis, Mitchell Wortsman, et al. Laion-5b: An open large-scale dataset for training next generation image-text models. *arXiv preprint arXiv:2210.08402*, 2022.
- [31] Chaehun Shin, Heeseung Kim, Che Hyun Lee, Sang-gil Lee, and Sungroh Yoon. Edit-a-video: Single video editing with object-aware consistency. *arXiv preprint arXiv:2303.07945*, 2023.
- [32] Uriel Singer, Adam Polyak, Thomas Hayes, Xi Yin, Jie An, Songyang Zhang, Qiyan Hu, Harry Yang, Oron Ashual, Oran Gafni, et al. Make-a-video: Text-to-video generation without text-video data. *arXiv preprint arXiv:2209.14792*, 2022.
- [33] Jiaming Song, Chenlin Meng, and Stefano Ermon. Denoising diffusion implicit models. *arXiv preprint arXiv:2010.02502*, 2020.
- [34] Narek Tumanyan, Michal Geyer, Shai Bagon, and Tali Dekel. Plug-and-play diffusion features for text-driven image-to-image translation. *arXiv preprint arXiv:2211.12572*, 2022.

- [35] Ruben Villegas, Mohammad Babaeizadeh, Pieter-Jan Kindermans, Hernan Moraldo, Han Zhang, Mohammad Taghi Saffar, Santiago Castro, Julius Kunze, and Dumitru Erhan. Phenaki: Variable length video generation from open domain textual description. *arXiv preprint arXiv:2210.02399*, 2022.
- [36] Wen Wang, Kangyang Xie, Zide Liu, Hao Chen, Yue Cao, Xinlong Wang, and Chunhua Shen. Zero-shot video editing using off-the-shelf image diffusion models. *arXiv preprint arXiv:2303.17599*, 2023.
- [37] Jay Zhangjie Wu, Yixiao Ge, Xintao Wang, Weixian Lei, Yuchao Gu, Wynne Hsu, Ying Shan, Xiaohu Qie, and Mike Zheng Shou. Tune-a-video: One-shot tuning of image diffusion models for text-to-video generation. *arXiv preprint arXiv:2212.11565*, 2022.
- [38] Saining Xie and Zhuowen Tu. Holistically-nested edge detection. In *Proceedings of the IEEE international conference on computer vision*, pages 1395–1403, 2015.
- [39] Jiarui Xu, Sifei Liu, Arash Vahdat, Wonmin Byeon, Xiaolong Wang, and Shalini De Mello. Open-vocabulary panoptic segmentation with text-to-image diffusion models. *ArXiv*, abs/2303.04803, 2023.
- [40] Jiahui Yu, Xin Li, Jing Yu Koh, Han Zhang, Ruoming Pang, James Qin, Alexander Ku, Yuanzhong Xu, Jason Baldridge, and Yonghui Wu. Vector-quantized image modeling with improved vqgan. *arXiv preprint arXiv:2110.04627*, 2021.
- [41] Lvmin Zhang and Maneesh Agrawala. Adding conditional control to text-to-image diffusion models. *arXiv preprint arXiv:2302.05543*, 2023.
- [42] Richard Zhang, Phillip Isola, Alexei A Efros, Eli Shechtman, and Oliver Wang. The unreasonable effectiveness of deep features as a perceptual metric. In *Proceedings of the IEEE conference on computer vision and pattern recognition*, pages 586–595, 2018.
- [43] Daquan Zhou, Weimin Wang, Hanshu Yan, Weiwei Lv, Yizhe Zhu, and Jiashi Feng. Magicvideo: Efficient video generation with latent diffusion models. *arXiv preprint arXiv:2211.11018*, 2022.
- [44] Xueyan Zou, Jianwei Yang, Hao Zhang, Feng Li, Linjie Li, Jianfeng Gao, and Yong Jae Lee. Segment everything everywhere all at once. *ArXiv*, abs/2304.06718, 2023.

A Experimental Setup

A.1 Semantic Metrics

Prompt Consistency. $\mathcal{C}_{\text{Prompt}}$ measures the average CLIP similarity between a target text query and each video frame, for all edited videos. For a unique pair (*image; caption*) the CLIP similarity writes: $CLIPScore(I, C) = \max(100 * \cos(E_I, E_C), 0)$ with E_I the visual CLIP embedding for an image I , and E_C the textual CLIP embedding for a caption C . The prompt consistency score then writes :

$$\mathcal{C}_{\text{Prompt}} = \frac{1}{N} \sum_{k=1}^N \frac{1}{F_k} \sum_{i=1}^{F_k} CLIPScore(V_i^k, C^k)$$

where V_i^k is the i th frame of video k , C^k the edited caption of video k , F_k the number of frames in video k and N the number of edited videos.

Frame Accuracy. $\mathcal{A}_{\text{Frame}}$ corresponds to average percentage of edited frames that have a higher CLIP similarity with the target text query than with their source caption, for all edited videos.

Directional Similarity. \mathcal{S}_{Dir} quantifies how closely the alterations made to an original image align with the changes between a source caption and a target caption. For a single edited frame the similarity score writes: $SIMScore(I_t, I_s, C_t, C_s) = 100 * \cos(E_{I_t} - E_{I_s}, E_{C_t} - E_{C_s})$ with E_{I_t} and E_{I_s} the visual CLIP embeddings of the edited image I_t and source image I_s , and E_{C_t} and E_{C_s} the textual CLIP embeddings of the edited caption C_t and source caption C_s . The global directional similarity score then writes:

$$\mathcal{S}_{\text{Dir}} = \frac{1}{N} \sum_{k=1}^N \frac{1}{F_k} \sum_{i=1}^{F_k} SIMScore(V_t^k, V_s^k, C_t^k, C_s^k)$$

with V_t^k and V_s^k the i th frame of the k th edited video and its source counterpart respectively and C_t^k, C_s^k their associated captions.

Frame Consistency. $\mathcal{C}_{\text{Frame}}$ is used to assess the temporal coherence of a video. It measures the CLIP similarity between consecutive video frames.

Aggregate Score. This metric synthesizes in a single score the overall performance of each model on semantic and similarity aspects, relatively to the best baseline. When dealing with metrics where a higher value is considered preferable, a coefficient in the aggregate score is computed as: $\max(\mathcal{S}_i) / \mathcal{S}_i^j$ i.e. the best score for metric i divided by the score of baseline j for metric i . When the objective is to minimize the metric, we take the inverse value. The minimal and best aggregate score for each aspect is 3, as we aggregate three semantic or similarity scores.

A.2 Similarity Metrics

Regarding content preservation, we have chosen three metrics that operate on different feature spaces in order to capture a rich description of perceptual similarities. **LPIPS** [42] operates on the deep feature space of a VGG network and has been shown to match human perception well. **HaarPSI** [28] operates on a wavelet space and shows the highest correlation with human opinion. Finally, **PSNR** assesses the distance between images directly at a pixel level. These metrics are extensively described in the literature and we refer to it for further details.

B Ablation Visualization

Fig. 8 illustrates the ablation study we led in Tab. 2. When VIDEEDIT receives both conditional controls, it produces high quality results. Conversely, when these controls are deactivated, the model is free to perform edits at random locations in the atlas, resulting in uninterpretable visual outcomes. Enabling only the edge conditioning yields similar results, with the difference that the model attempts to locally match inner and outer edges. Finally, the sole use of a mask allows to perform edits at the correct locations, but that are semantically absurd once mapped back to the image space.



Figure 8: Ablation visualization.

C Additional Results

C.1 VIDEEDIT samples

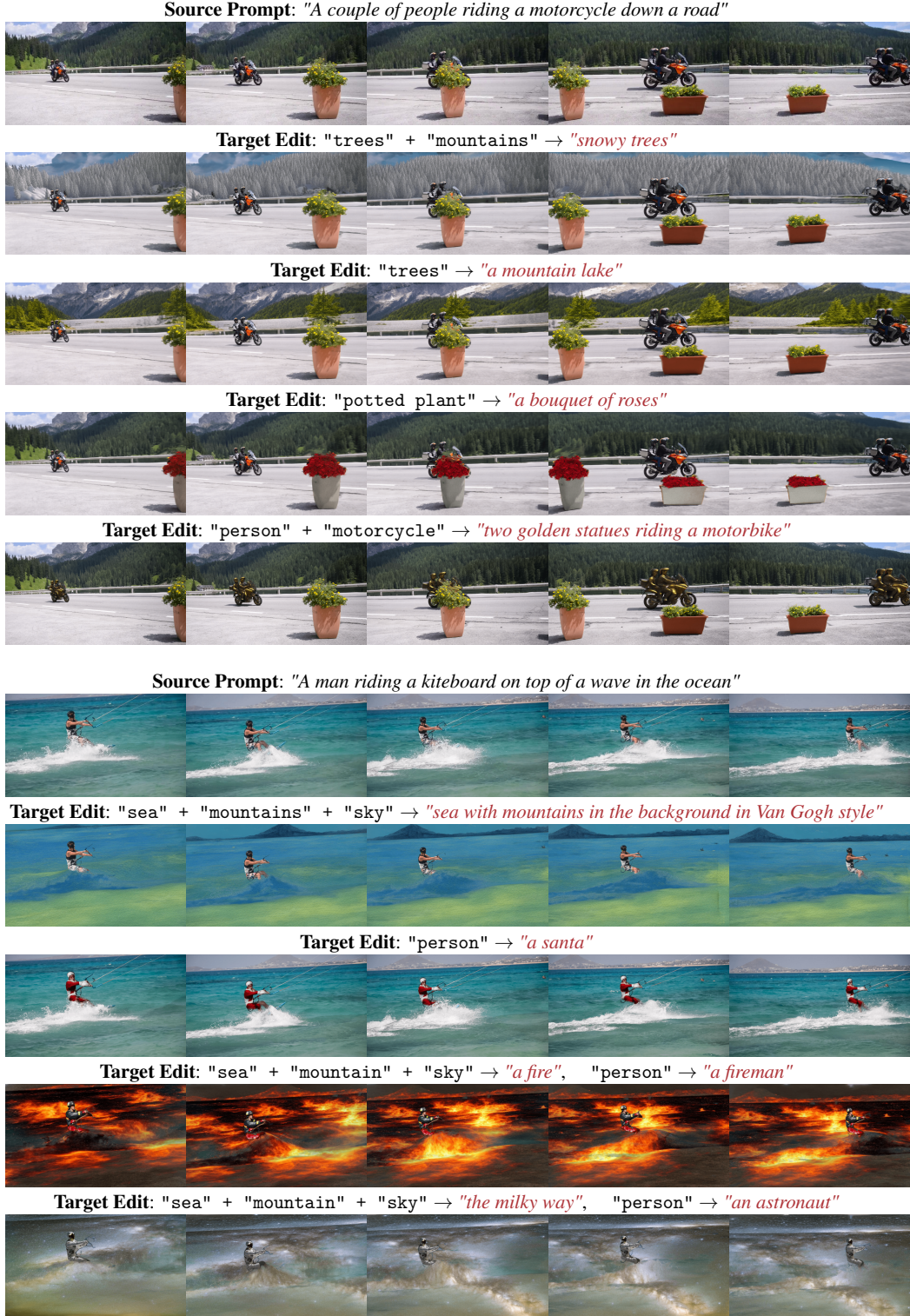


Figure 9: Additional VIDEEDIT sample results.

C.2 Baselines Comparison

Fig. 10 shows additional baselines comparison examples. We can see on both videos that VIDEEDIT renders more realistic and higher quality textures than other methods while perfectly preserving the original content outside the regions of interest. The flamingo has subtle grooves on its body that imitate feathers and a fine light effect enhances the edit’s grain. On the contrary, Text2Live struggles to render a detailed plastic appearance. The generated wooden boat also looks less natural and more tarnished than VIDEEDIT’s. Tune-a-Video and Pix2Video render unconvincing edits and completely alters the original content.

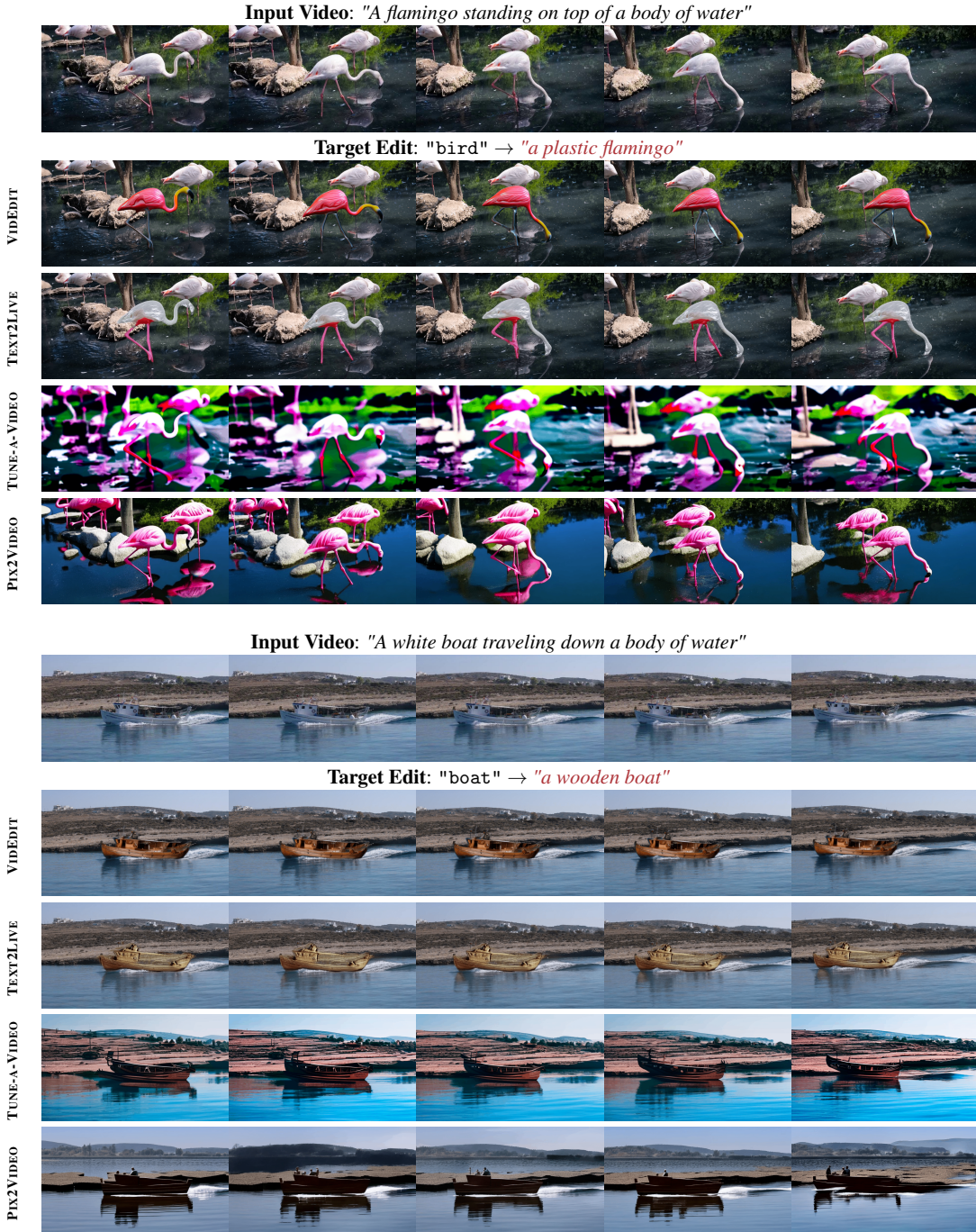


Figure 10: Additional qualitative comparison between baselines.

D Blending Effect

Fig. 11 shows the blending step’s importance in the editing pipeline (Fig. 3). When considering only the RGB channels of a foreground atlas to infer an object’s mask, the segmentation network has to deal with low contrasts between the background and the object, as well as duplicated representations within the overall atlas representation. This might lead to partially detected objects or masks placed at an incorrect location. In order to avoid these pitfalls, we leverage the atlas’ alpha channel which indicates which pixels contain relevant information and must thus be visible. Therefore, we choose to blend the RGB channels with a fully white image according to the alpha values:

$$\mathbb{A}_{\text{Blended}} = \mathbb{A}_{\text{RGB}} \odot \alpha + \mathbb{I} \odot (1 - \alpha)$$

with \mathbb{A}_{RGB} the RGB channels of an atlas representation, \mathbb{I} a fully white image and α the atlas’ opacity values.

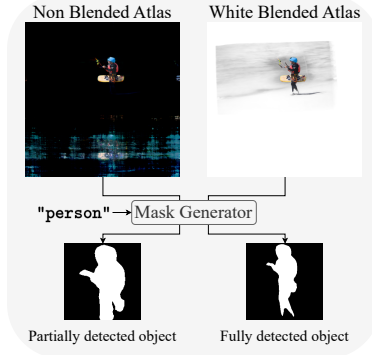


Figure 11: Alpha blending effect

E Editing Time

Focusing on the interactive part of editing³ in which users are interested in⁴, Figure 12 underlines the lightweight aspect of our method. The panel on the left shows that VIDEEDIT can perform a large number of edits on a 70 frame long video in significantly less time than other approaches. As an illustration, VIDEEDIT demonstrates approximately 30 times faster editing capabilities compared to Text2Live, which is the second leading baseline in terms of editing capacities. On the other hand, as depicted in the right panel, the use of VIDEEDIT becomes increasingly time-efficient compared to other baselines, as the number of frames to edit grows.

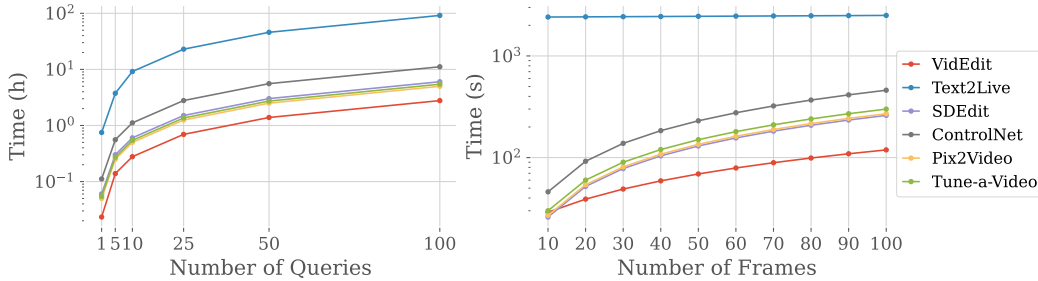


Figure 12: **Editing time.** VIDEEDIT can edit videos significantly faster than existing methods.

³Steps as DDIM inversion or LNA construction being considered as pre-processing steps.

⁴Editing the atlas and reconstructing the video for atlas based methods. Simply inferring the model for other baselines.